Molecular basis of ligand recognition by OASS from E-histolytica: Insights from structural and molecular dynamics simulation studies

ARTICLE *in* BIOCHIMICA ET BIOPHYSICA ACTA · JUNE 2013

Impact Factor: 4.66 · DOI: 10.1016/j.bbagen.2013.05.041 · Source: PubMed

3 AUTHORS:

Isha Raj
Jawaharlal Nehru University
11 PUBLICATIONS **68** CITATIONS
SEE PROFILE

Mohit Mazumder
Jawaharlal Nehru University
14 PUBLICATIONS **17** CITATIONS
SEE PROFILE

Samudrala Gourinath
Jawaharlal Nehru University
64 PUBLICATIONS **766** CITATIONS
SEE PROFILE

Biochimica et Biophysica Acta 1830 (2013) 4573–4583

Contents lists available at SciVerse ScienceDirect

Biochimica et Biophysica Acta

journal homepage: www.elsevier.com/locate/bbagen

Molecular basis of ligand recognition by OASS from *E. histolytica*: Insights from structural and molecular dynamics simulation studies

Isha Raj, Mohit Mazumder, Samudrala Gourinath *

School of Life Sciences, Jawaharlal Nehru University, New Delhi 110067, India

ARTICLE INFO

Article history:
Received 26 February 2013
Received in revised form 8 May 2013
Accepted 29 May 2013
Available online 6 June 2013

Keywords:
Cysteine biosynthetic pathway
O-acetyl serine sulfhydrylase
Active site cleft
Inhibition
Ligand binding
Conformational change

ABSTRACT

Background: O-acetyl serine sulfhydrylase (OASS) is a pyridoxal phosphate (PLP) dependent enzyme catalyzing the last step of the cysteine biosynthetic pathway. Here we analyze and investigate the factors responsible for recognition and different conformational changes accompanying the binding of various ligands to OASS.
Methods: X ray crystallography was used to determine the structures of OASS from *Entamoeba histolytica* in complex with methionine (substrate analog), isoleucine (inhibitor) and an inhibitory tetra-peptide to 2.00 Å, 2.03 Å and 1.87 Å resolutions, respectively. Molecular dynamics simulations were used to investigate the reasons responsible for the extent of domain movement and cleft closure of the enzyme in presence of different ligands.
Results: Here we report for the first time an OASS-methionine structure with an unmutated catalytic lysine at the active site. This is also the first OASS structure with a closed active site lacking external aldimine formation. The OASS-isoleucine structure shows the active site cleft in open state. Molecular dynamics studies indicate that cofactor PLP, N88 and G192 form a triad of energy contributors to close the active site upon ligand binding and orientation of the Schiff base forming nitrogen of the ligand is critical for this interaction.
Conclusions: Methionine proves to be a better binder to OASS than isoleucine. The β branching of isoleucine does not allow it to reorient itself in suitable conformation near PLP to cause active site closure.
General significance: Our findings have important implications in designing better inhibitors against OASS across all pathogenic microbial species.

1. Introduction

Growth and survival of the protozoan parasite *Entamoeba histolytica* are critically dependent upon the cysteine biosynthetic pathway. Cysteine, which is the product of this pathway, is the only anti-oxidative thiol in *Entamoeba histolytica* and plays an important role in maintaining the redox balance in this organism [1]. This amino acid is important for optimal growth of *Entamoeba* and is essential for its attachment and survival under oxidative stress [2–6].

The de novo cysteine biosynthetic pathway starts with serine acetyl transferase (SAT, EC 2.3.1.30) catalyzing the formation of O-acetyl serine (OAS) from acetyl Co-A and serine. OAS is then converted to cysteine by the addition of sulfide and elimination of acetate in a reaction catalyzed by O-acetyl serine sulfhydrylase (OASS, EC 2.5.1.47). OASS follows a ping pong kinetic mechanism where the conserved catalytic lysine residue forms an internal aldimine with PLP in the native state. OAS substitutes for lysine at the active site and forms an external Schiff base with PLP, followed by β elimination in which acetate is released and a proton is abstracted from the α position [7]. This leads to the formation of the α amino acrylate intermediate covalently linked to PLP (Fig. 1). Nucleophilic attack of the second substrate, sulfide, on the β carbon of the amino acrylate intermediate re-protonates the α carbon, resulting in cysteine bound as an external Schiff base. The product is then released, restoring the internal aldimine.

The structure of OASS from *E. histolytica* (EhOASS) in its native (i.e unmutated/unliganded) form, as well as with cysteine bound, has been reported [8]. The conformation of EhOASS belongs to the type II fold of PLP dependent enzymes [9,10], similar to that in other plant and bacterial OASSs [11–14]. Structural and biochemical studies have shown that in addition to the substrate OAS, OASS can bind to cysteine, its product, and to methionine, a substrate analog [8,14,15]. OASS activity is regulated both by its metabolites and by interaction with SAT, the other enzyme of the cysteine biosynthetic pathway. The SAT C-terminal peptide has been shown to interact with the OASS active site to inhibit its activity [16–19]. The common feature of all these SATs is the presence of a conserved Ile at its C-terminal end. Cysteine synthase complex does not form in *E. histolytica*, despite the presence of isoleucine at the C-terminal end of SAT1 in this organism [20].

Earlier studies to determine the conformational changes taking place upon substrate binding have mostly employed methionine as a substrate analog and a modified OASS, where the catalytic Lys was mutated to Ala. The structure of an OASS K41A mutant from *Salmonella typhimurium* in complex with methionine revealed methionine bound in an external aldimine (EA) linkage with PLP and accompanied with

* Corresponding author. Tel.: +91 11 26704513; fax: +91 11 26187338.
E-mail address: sgourinath@mail.jnu.ac.in (S. Gourinath).

0304-4165/$ – see front matter © 2013 Elsevier B.V. All rights reserved.
http://dx.doi.org/10.1016/j.bbagen.2013.05.041

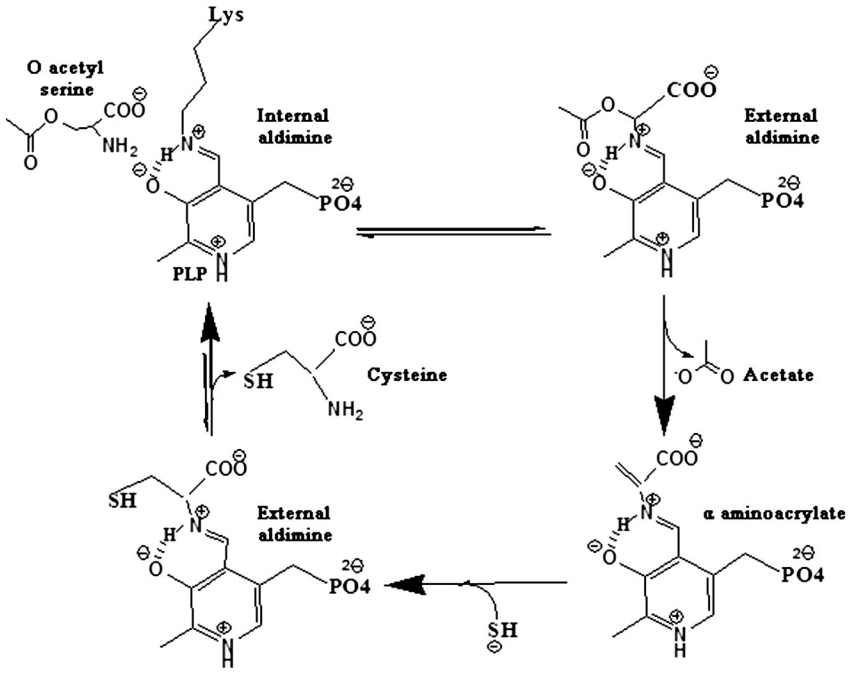

Fig. 1. Reaction mechanism of OASS. The overall catalytic cycle is shown in four steps.

a large conformational change leading to closure of the active site [15]. However the corresponding structure determination of OASS K46A from *Arabidopsis thaliana* showed that the enzyme remains in the open conformation even after formation of the EA between methionine and PLP [14]. Another structure of OASS, from *Mycobacterium tuberculosis* bound to the α aminoacrylate intermediate, also showed a closed active site [21]. It is not clear why the active site cleft is open in one case and closed in other cases even though the EA is formed in all the cases. A comparison of the protein sequences of these three OASSs with EhOASS reveal conserved residues at the active site (Supplementary Fig. 1) but it was also shown that the OASS active site cleft is widest in *E. histolytica*, which could be a reason for the lack of formation of a cysteine synthase complex in this organism [22]. In view of the importance of cysteine in *E. histolytica*, OASS could be a good drug target as OASS homologues are absent in mammalian hosts and therefore an understanding of the finer details of recognition of substrate and inhibitor by the enzyme is important. The substrate OAS, substrate analog Met, Product Cys and inhibitor Ile structure are shown in Supplementary Fig. 2. The role of isoleucine as an inhibitor of OASS has been studied by inhibitory SAT C-terminal peptides [22]. So far drugs have been designed based on open conformation of OASS (isoleucine or peptide as a template) [19,35,36], which yielded only micro-molar binding affinity inhibitors. Here for the first time we present a structure of EhOASS with a substrate analog. Unlike previous OASS complex structures, an external aldimine in EhOASS is not formed and yet the active site is in a closed conformation when methionine is bound. We also report the structure of EhOASS in complex with the inhibitor isoleucine, which is also the first time any OASS structure with isoleucine bound has been reported. In addition, this study also reports the structure of EhOASS with the EhSAT1 C-terminal tetra-peptide, SPSI. EhOASS is in a closed conformation when bound to methionine, and in an open conformation when bound to either isoleucine or the peptide. Based on the structural information, computational studies were performed to provide further insights into molecular recognition between EhOASS and its substrate or inhibitor. Molecular dynamics simulations on the EhOASS-methionine complex and EhOASS-isoleucine complex structures identified the hot spot residues critical for ligand binding. Since these residues are conserved in OASS from organisms across species (Supplementary Fig. 1), our findings are applicable to the general mechanism of OASS activity. The present study suggests that designing inhibitors based on closed conformation/methionine could result in better inhibitors then those based on isoleucine or SAT C-terminal mimicking peptides.

2. Materials and methods

2.1. Co-crystallization of EhOASS with methionine, isoleucine and EhSAT1 derived C-terminal peptide SPSI

*Eh*OASS was expressed and purified as reported earlier [23]. Purified and concentrated EhOASS (11.5 mg/ml) was mixed separately with either methionine, isoleucine or the peptide SPSI so that the final concentration of each ligand was 10 mM in the protein-ligand mix. Each mixture was incubated for 1 h at room temperature (RT) prior to crystallization. The *Eh*OASS complexes were crystallized in hanging drops by mixing equal volumes (2 μl) of protein with a precipitant solution containing 2.15 M ammonium sulfate, 100 mM Tris, pH 6.6 to 7.2 at 289 K.

2.2. Data collection, processing and structure determination of crystals of EhOASS in complex with ligand

For the X-ray diffraction experiments, EhOASS complex crystals were washed with successively increasing amount of glycerol in mother liquor, from 5% to 15%, for cryo-protection. The crystals were then mounted on cryoloops and flash frozen in liquid nitrogen. These crystals diffracted to 1.8 Å resolution for *Eh*OASS-methionine and EhOASS-SPSI complexes and to 2.0 Å resolution for EhOASS-isoleucine with an in-house rotating anode generator (At NII or AIRF, JNU New Delhi). Each of these complexes crystallized in space group P41 (Table 1) with two molecules per asymmetric unit. The data were indexed, integrated and scaled using Automar software [24].

The EhOASS-methionine structure was determined by molecular replacement using the EhOASS-cysteine bound structure, 3BM5 [8], as a search model for MolRep [25]; the best solution had a correlation coefficient of 0.70 and an R-factor of 35.2%. The EhOASS-isoleucine and EhOASS-SPSI structures were also solved using MolRep, but the search model for them was the EhOASS native structure, 2PQM [8]. The resulting structures were subjected to alternate restrained refinement

using Refmac5 [26] and manual fitting to the electron density with the help of COOT [27]. The PLP molecule and sulfate were added manually, guided by Fo–Fc electron density at $>3\sigma$ contour level. The large Fo–Fc density at the active site was a clear indication of bound methionine and isoleucine at the active sites of the respective structures. However, in the SPSI bound EhOASS structure, only the first two amino acid residues of the tetra peptide ligand could be traced into the density; the disorder of the last two residues (Ser and Pro) is consistent with the very weak binding of SPSI for EhOASS. Water molecules were initially picked using the COOT graphics package and then later checked by considering electron density and H-bonding interactions. The final refined EhOASS-Met, EhOASS-Ile and EhOASS-SPSI structures yielded R factors of 18.1, 19.1 and 18.4 respectively (Table 1).

2.3. Molecular dynamics (MD) simulations of EhOASS-Met and EhOASS-Ile structures

To understand cleft closure upon ligand binding, the crystal structures of the complexes of OASS with methionine and isoleucine were subjected to molecular dynamics simulations. Parameters for LLP (catalytic lysine covalently linked to PLP) were generated using antechamber module of AMBER suite [28]. The restrained electrostatic potential (RESP) was used to describe the partial atomic charges. Then the general AMBER force field (GAFF) [29] was used to describe the parameters of LLP. The standard AMBER force field for bioorganic systems (ff03) [30] was employed to describe the protein, followed by the addition of hydrogen atoms and counter ions to neutralize the system. The input files for energy minimization, dynamics and analysis were prepared with xleap. Both systems were solvated using atomistic TIP3P water in a box with edges at least 12 Å from the complex.

All simulations were performed using AMBER molecular dynamics suite version 9 [28] Energy minimization was first conducted with the steepest descent method and then switched to conjugate gradient every 500 steps for a total of 5000 steps with 0.1 kcal/mol $Å^2$ restraints on all atoms of the complexes. Following this step, another two rounds of energy minimization were performed by only restraining the protein and further releasing all the restraints for 2000 steps of each round. Long-range Coulombic interactions were handled using the particle mesh Ewald (PME) summation [31]. For the equilibration and subsequent production runs, the SHAKE algorithm was employed on all atoms covalently bonded to a hydrogen atom, allowing for an integration time step of 2 fs. The system was gently annealed from 0 K to 300 K over a period of 50 ps using a Langevin thermostat with a coupling coefficient of 1.0 ps and 50 ps of density equilibration with weak restraints. The system was again equilibrated for 500 ps without any restrains. The production phase of the simulations was run without any restraints for a total of 20 ns on each system. Coordinates and energy values were collected every 10 ps throughout the simulations.

2.4. Binding free energy calculations (MM/PB (GB) SA)

The binding free energies of OASS for methionine and for isoleucine were analyzed by the MM/PB (GB) SA scripts, integrated in the AMBER 11 software package [28]. In this procedure, snapshots were first extracted from the obtained trajectories. For each snapshot, the free energy is calculated for the protein, ligand, and complex using single trajectory approach. The binding free energy is computed as the difference:

$$\Delta G_{bind} = G_{complex} - G_{protein} - G_{ligand}.$$

2.5. Per residue interaction decomposition

To determine the contribution of each residue to the binding energy, the MM-GBSA method [32] was used. MM-GBSA method decomposes the interaction energies for each residue by considering molecular mechanics and solvation energies without consideration of the contribution of entropies. Each residue contribution includes three terms: van der Waals contribution (ΔG_{vdw}), electrostatic contribution (ΔG_{ele}) in a vacuum and solvation contribution ($\Delta G_{solvation}$).

$$\Delta G_{residue} = \Delta G_{vdw} + \Delta G_{ele} + \Delta G_{solvation}.$$

All energy components in above equation were calculated using 1000 snapshots from the last 10 ns of the MD simulation.

Table 1
Crystallographic data-statistics of EhOASS complexes.
Values in parentheses are for the last resolution shell.
Free R factor was calculated with a subset of 5% randomly selected reflections.

Data Set	EhOASS + Met	EhOASS + Ile	EhOASS + SPSI
Crystallographic data			
X-ray source	RigakuMicroMAX		BrukerMicrostar
Wavelength (Å)	1.54	1.54	1.54
Space group	$P4_1$	$P4_1$	$P4_1$
Unit cell parameters (Å)	A = B = 80.41, C = 112.23	A = B = 80.4, C = 112.14	A = B = 80.58, C = 112.63
Resolution range(Å)	30-1.86	30-2.03	30-1.86
R_{sym}(%)	3.9(16.2)	3.2(12.9)	2.7(14.3)
Completeness	97.5	99.5	98.8
Total no. of observations	263,029	176,181	235,657
No. of unique observations	57,214	45,128	58,947
Redundancy	5.4(5.3)	3.9(3.7)	3.9(3.6)
Average I/s(I)	10(3.4)	11.2(3.7)	13.5(3.2)
Crystal mosaicity (°)	0.33	0.38	0.36
Refinement		Resolution	1.8
2.0	1.86		
R_factor (%)	17.7	19.1	18.4
Free_R factor (%)	21.9	23.8	21.3
Mean B_factor	24.9	26.4	27.5
Number of atoms			
Protein/water/sulfate/other	5147/353/2/9	5073/312/2/9	5145/320/2/19
RMS deviations		Bonds (Å)	0.026
0.029	0.031	Bond angles (°)	2.081
2.12	2.27		
ESU based on Free_R (Å)	0.161	0.132	0.128

Co-ordinates and structure factors for EhOASS bound with isoleucine, methionine and SAT derived tetrapeptide, SPSI, have been deposited in the protein data bank with accession id 4IL5, 4JBL and 4JBN respectively.

3. Results and discussion

3.1. Structure of EhOASS in complex with methionine

The crystal structure of EhOASS with substrate analog methionine revealed a few unexpected features. The EhOASS-methionine complex crystallized as a dimer in the space group $P4_1$ (Table 1), but methionine was found to be bound to only one of the monomers. This is consistent with the observation of only the monomer with bound methionine has a closed active site, whereas the other monomer shows an open active site. Methionine is seen bound in the active site cleft between the N-terminal domain and the C-terminal domain, very close to PLP as depicted in Fig. 2A. Earlier reports had shown that EhOASS binds to methionine forming an EA as can be seen by the shift in the λ_{max} or peak absorption of EhOASS from 412 nm to 418 nm. There is also a change in the absorption spectrum for EhOASS at 470 nm as the concentration of methionine changes [8]. Our titration experiment using fluorescence showed that Met has a Kd of around 0.5 mM with EhOASS (Supplementary Fig. 3). Based on this observation we expected to find methionine in an EA linkage at the active site in the EhOASS-methionine complex. However, no electron density for the EA linkage with PLP could be detected (Fig. 2A inset) despite the active site being closed in the methionine bound structure. The side chain of methionine is directed towards the active site entrance while the nitrogen of its amino group faces PLP. The potential Schiff base forming nitrogen of LLP is about 3 Å from methionine's amino nitrogen, resulting in hydrogen bond formation between the two atoms. This interaction could subsequently lead to the abstraction of a proton and thereby formation of the EA with methionine, but in the present structure PLP remains in an internal Schiff base with Lys 58. Earlier attempts to crystallize OASS with the substrate analog methionine in *S. typhimurium* [15] and *A. thaliana* [14] employed active site mutants where the catalytic lysine residue was replaced with alanine. In these cases a methionine from the media interacted with the PLP at the active site to form an EA linkage.

The formation of EA linkage though does not ascertain conformational change in the enzyme to close the active site (Table 2). For OASSs from *S. typhimurium* (StOASS) and *A. thaliana* (AtOASS) in complex with methionine, it was found that, although EA is formed in both cases, only in StOASS is it accompanied with a large conformational change leading to active site closure; the AtOASS structure retains an open conformation [14,15]. In the α-aminoacrylate intermediate bound structure of OASS from *M. tuberculosis* (MtOASS), the active site is closed. However, despite the lack of EA formation in the EhOASS-methionine

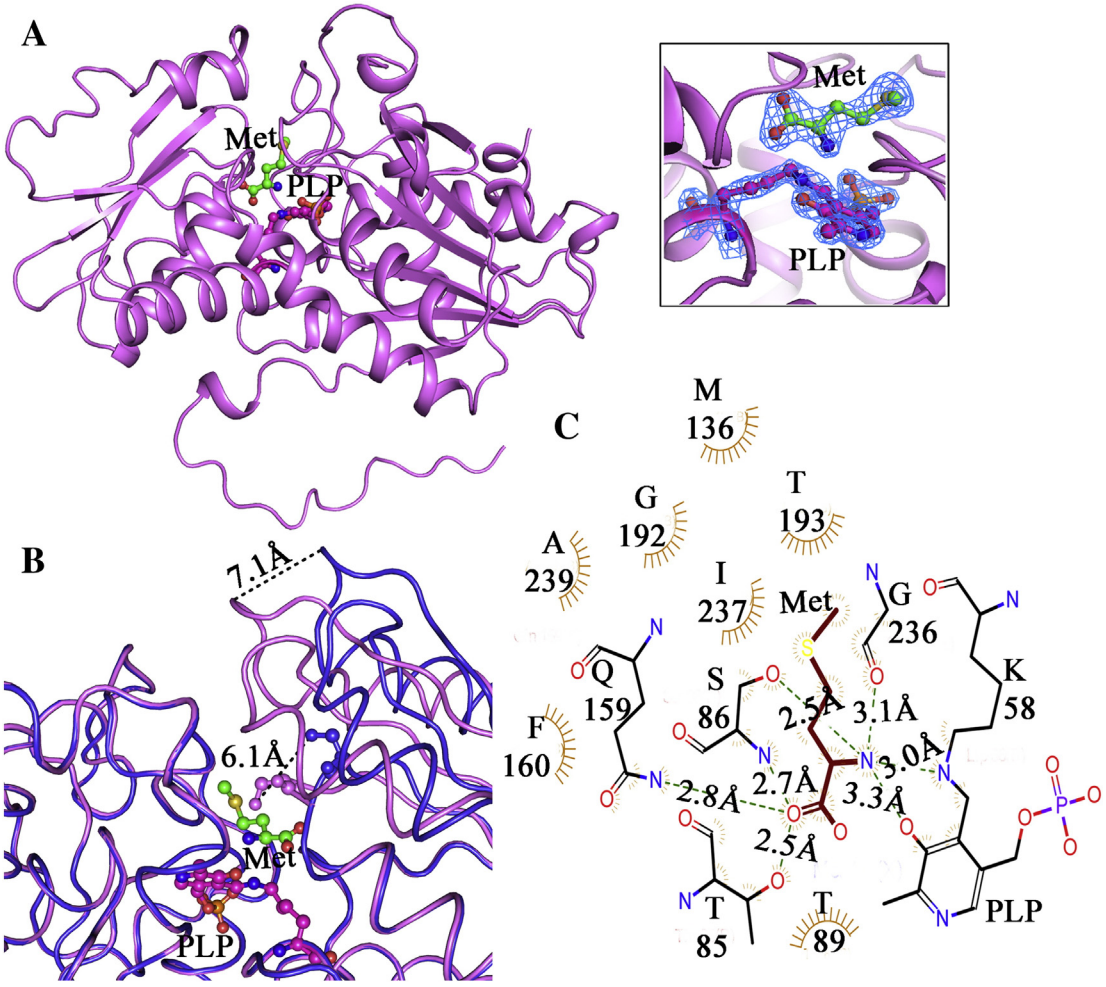

Fig. 2. EhOASS in complex with methionine and its interaction at the active site. (A.) Methionine (represented by green balls and sticks) is bound near PLP at the active site cleft between N-terminal domain and C-terminal domain. Inset shows the difference Fourier electron density map (2Fo–Fc) at 2σ cut-off for methionine, cofactor PLP and catalytic lysine. (B.) Superimposition of EhOASS-methionine bound monomer(magenta) over the other monomer of the asymmetric unit in which methionine is not bound (blue), revealing the movement of N-terminal domain in the methionine-complexed monomer. Residue Ser86 of the conserved Asn loop, shown as sticks, shows the maximum displacement within the loop. (C.) LIGPLOT of the interactions of methionine with the residues of EhOASS at the active site. The Asn loop, 85TSGNT89 and the Gly loop, 236GIGA239, together play an important role in these interactions.

Table 2
Comparison of ligand bound structures of OASS from various organisms on the basis of external aldimine formation and active site cleft closure (EA—external aldimine, ASC—active site cleft). The C–N distance indicates the distance between aldimine forming C4A from PLP and N from the ligand. The distance indicated in the brackets is the distance between C4A of PLP and NZ of the catalytic lysine.

Organism	α Aminoacrylate			Methionine			Cysteine		
	EA	ASC	C–N distance	EA	ASC	C–N distance	EA	ASC	C–N distance
E. histolytica	nd	–		No	Closed	3.3 Å (1.4 Å)	Yes	Closed	2.4 Å (1.8 Å)
A. thaliana(K46A)*	nd	–		Yes	Open	1.3 Å	nd	–	
S. typhimurium(K41A)*	nd	–		Yes	Closed	1.4 Å	nd	–	
M. tuberculosis	Yes	Closed	1.4 Å (4.0 Å)	nd	–		nd	–	

* Catalytic lysine has been mutated to ala in these structures (nd—such structures have not been determined).

structure, methionine forms a network of hydrogen bonds with the conserved residues surrounding the active site (Fig. 2C), resulting in the movement of the N-terminal domain by almost 7 Å in comparison to the native EhOASS structure and hence resulting in the closure of the active site (Fig. 2B). The majority of the hydrogen bonding interactions come from two conserved loops: the Asn loop (85TSGNT89) from the N-terminal domain and the Gly loop (236GIGA239) from the C-terminal domain (Supplementary Table 1).

3.2. Structure of EhOASS in complex with isoleucine and EhSAT1 derived tetra-peptide SPSI

Previous structural and biochemical studies of OASS and SAT from *Haemophilus influenzae*, *A. thaliana* revealed that the C-terminal residues of SAT, and specifically the conserved isoleucine at the C-terminal end, play an important role in interacting with the active site of OASS [16,33,34]. It is also known that this interaction is inhibitory in nature to OASS. We tried to determine the Kd of isoleucine with EhOASS through biochemical experiments, which does not affect PLP fluorescence therefore we could not determine its Kd. In order to determine the mode of interaction of isoleucine with the EhOASS active site, we co-crystallized isoleucine with EhOASS and obtained a complex that diffracted to 2.0 Å resolution (Table 1). As is the case for methionine, isoleucine is also bound to only one of the active sites of the dimer. Moreover, the electron density reveals that isoleucine binds at a similar location (albeit with low sigma cutoff) in the active site as does methionine, i.e. between the N-terminal and C-terminal domains near PLP (Fig. 3A). However, unlike the methionine-bound structure, there is no closure of the active site in this case. The amino nitrogen of isoleucine does not face the cofactor PLP, but instead faces the active site cleft opening, as does the isoleucine side chain (Fig. 3A). Isoleucine seems to be tethered to the active site mainly through H-bonding interactions between its α—carboxylate group and the Asn loop (Fig. 3B).

The crystallographic analysis of EhOASS complexed with EhSAT1 derived C-terminal tetra peptide, SPSI, also revealed (some) electron density for the ligand in only one monomer at the active site. For ease of discussion, the amino acid residues in the peptide are numbered from the C-terminus: 1-Ile, 2-Ser, 3-Pro, 4-Ser. Only the 1st and 2nd amino acid residues, Ile and Ser, could be traced into the electron density with confidence. The 3rd residue, Pro, was modeled as an Ala into the poorly ordered density at its location (Fig. 3D). We could not model the 4th residue into this density. The incomplete and relatively weak electron density for the tetra peptide at the active site is consistent with the poor binding of SPSI for EhOASS. In fact, EhSAT1 is unable to bind to EhOASS, and the peptide itself does not give proper signals upon fluorescence titrations and ITC titrations (Supplementary Fig. 4). When the 3rd and 4th amino acid residues were changed to large hydrophobic amino acids (Trp or Phe or Tyr) and Asp respectively, the peptide binds strongly to EhOASS [17].

The interactions made by the peptide SPSI at the active site are similar to those made by isoleucine at the active site. The terminal Ile from the peptide and the free isoleucine assume very similar conformations, i.e., the N from the amino group of both isoleucines face away from catalytic LLP. However, there is a slight change in the orientation of the side chain of the isoleucines in the two structures. The free isoleucine is bound at the active site with its gamma methyl group facing the cofactor. In the peptide bound structure, the delta methyl group of Ile faces the cofactor PLP, while the rest of this residue's atoms along with other residues of the peptide face away from it into the opening of the active site cleft (Fig. 3E). Analysis of the potential H-bonding residues of the EhOASS active site and those of the peptide revealed that major interactions are made between the terminal Ile of the peptide and the Asn loop, Gly loop, the conserved Gln 159, Gly 192 and Thr 193 residues of the protein. Besides the similar interactions made by the common isoleucine, only three additional potential H-bonds could be formed by the two extra ordered amino acid residues of the peptide (Supplementary Table 2 and supplementary Table 3).

A comparison of the residues involved in H-bonding in the EhOASS-peptide structure with other peptide structures from other organisms shows that *E. histolytica* is unique in having only the terminal Ile of the peptide involved in extensive interactions with the protein. For HiOASS(OASS from *H. influenzae*)[19], AtOASS [16] and LdOASS (OASS from *Leishmania donovani*) [22], there are significant contributions to the interactions made by other residues of the peptide too. The large size of the EhOASS active site cleft [22] may be the cause of the poor binding of EhSAT1 derived C-terminal peptide to EhOASS and by extension the absence of a cysteine synthase complex in *E. histolytica* [22].

3.3. Detailed comparisons with ligand bound OASS structures from other sources

The EhOASS-methionine structure is very similar to other closed cleft OASS structures. The methionine bound monomer has an RMSD of 0.583 Å with MtOASS-α aminoacrylate structure [21], based on the superimposition of 244 Cα atoms, an RMSD of 0.682 Å with AtOASS(K46A mutant)-methionine bound structure [14] for 244 Cα atoms, and an RMSD of 0.666 Å with StOASS(K41A mutant)-methionine structure [15] for 225 atoms. With its native structure and cysteine bound structure, EhOASS-methionine structure has RMSD of 0.163 Å and 0.118 Å respectively for 272 atoms. If we compare just the N-terminal domain, then for 71 atoms the RMSD with the native structure is 1.194 Å while that with the cysteine bound structure is 0.511 Å. As observed in the StOASS-methionine structure and the MtOASS-α aminoacrylate intermediate bound structure, the largest conformational changes, compared to their unliganded structures, occur in the Asn loop, 85TSGNT89. The N-terminal domain appears to flex about Leu 75, rotating the region from this residue to Lys 153 between the open and closed cleft conformations. The maximum displacement occurs in the Asn loop, particularly Ser 86, which shifts by 6.1 Å to make contacts with methionine at the active site. Almost all structures with reaction intermediates or substrate analog report a rotation in the cofactor ring plane (6° in StOASS-met structure, 19° in MtOASS-α aminoacrylate intermediate structure) to facilitate the formation of EA. However, we found a maximum rotation of only about 1° in the PLP ring in our methionine bound structure compared to native and isoleucine or SPSI bound EhOASS structures. This indicates

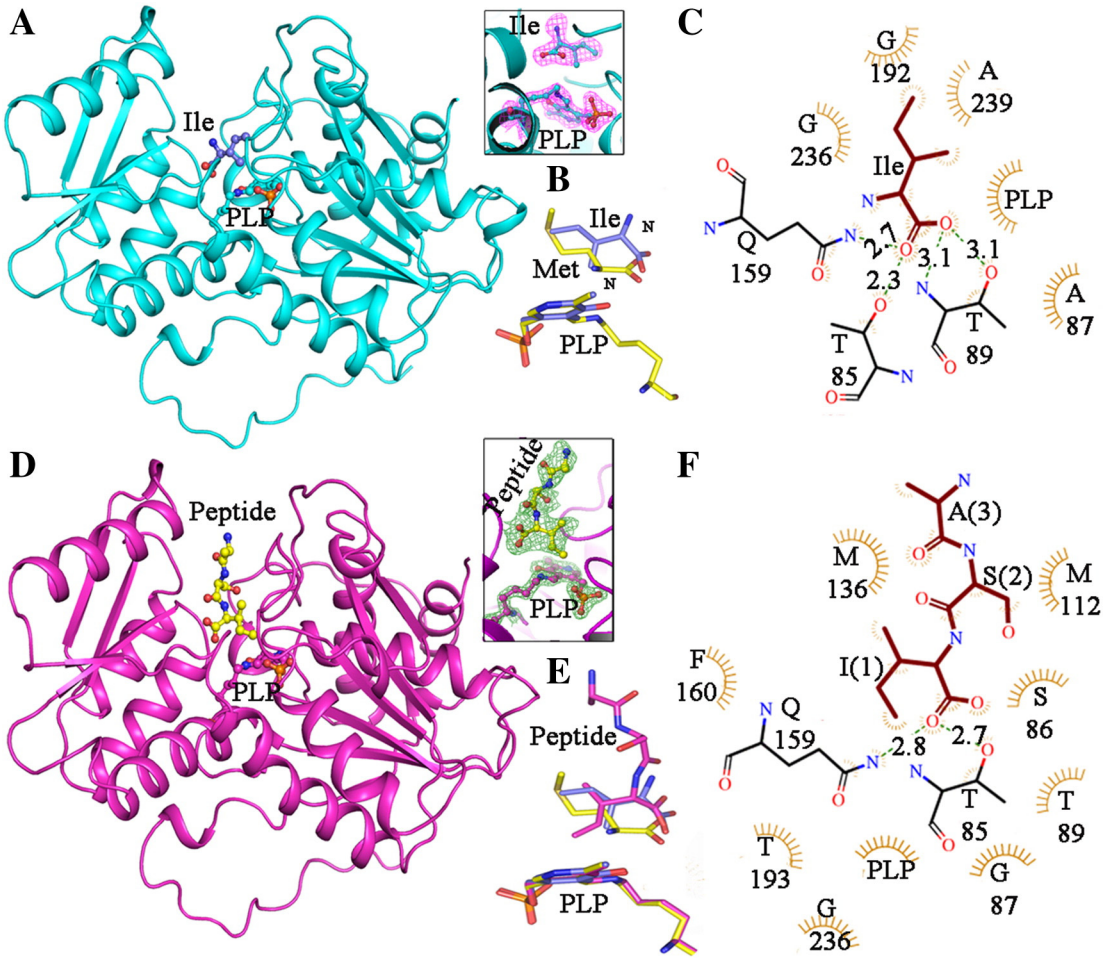

Fig. 3. EhOASS in complex with isoleucine and tetrapeptide and their interactions at the active site. (A.) Isoleucine (represented by blue balls and sticks) is bound near PLP at the active site cleft between N-terminal domain and C-terminal domain. Inset shows the difference Fourier electron density map (2Fo–Fc) at 1.5σ cutoff for isoleucine, and 2σ cutoff for cofactor PLP and catalytic lysine. (B.) Superimposition with methionine at the active site reveals the difference in orientation of N in isoleucine away from cofactor PLP. (C.) LIGPLOT of the interactions of isoleucine with residues at the EhOASS active site. (D.) The EhOASS monomer with bound SPSI (represented by yellow balls and sticks) at the active site cleft between N-terminal domain and C-terminal domain. Inset shows the difference Fourier electron density map (2Fo–Fc) at 1.2 σ cutoff for SPSI, and 2σ cutoff for cofactor PLP and catalytic lysine. (E.) Superimposition with methionine (yellow) and isoleucine (blue) at the active site reveals the difference in the orientation of N and the side chain. The peptide is depicted in pink. (F.) LIGPLOT of the interactions of peptide with residues at the EhOASS active site.

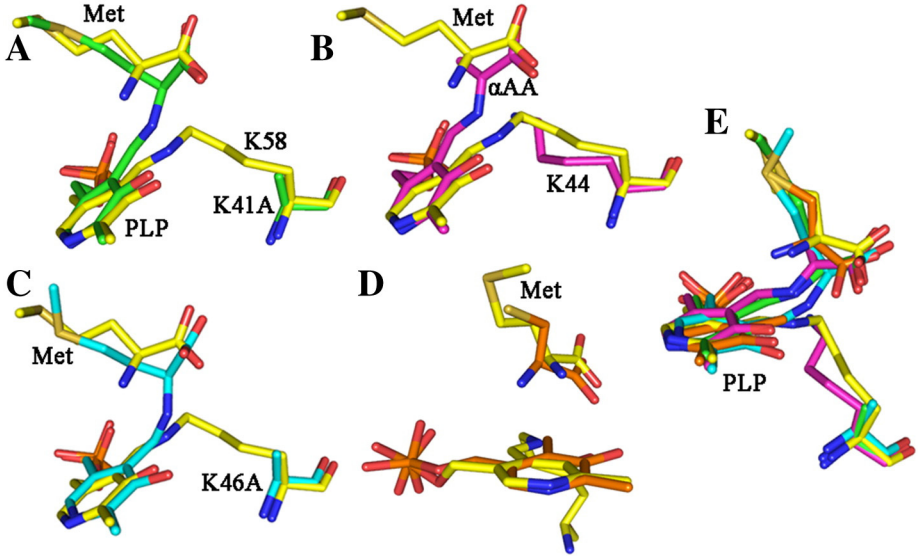

Fig. 4. Superimposition of intermediates with the cofactor PLP at the active site of various OASS Structures. Superimposition of EhOASS-methionine depicted in yellow with (A.) StOASS-methionine EA, depicted in green (B.) MtOASS-αAA, depicted in pink (C.) AtOASS-methionine EA, depicted in cyan (D.) EhOASS-cysteine, depicted in orange and (E.) superimposition of all these structures. Abbreviations: EA—external aldimine, αAA—αaminoacrylate.

Table 3
The binding free energy of EhOASS met and Ile bound complexes. The table shows the detailed contribution of energy components calculated using Poisson Boltzmann Surface Area (MM-PBSA) method for EhOASS methionine and isoleucine bound complexes to evaluate their binding activity. Here ΔE_{Ele}, electrostatic interactions; ΔE_{Vdw}, van der Waals interactions, $\Delta E_{MM} = \Delta E_{Ele} + \Delta E_{Vdw}$,$\Delta G_{sol-ele}$: polar solvation free energy are calculated by solving the Poisson–Boltzmann equation PB; ΔG_{sol-np}, non-polar solvation free energy, $\Delta G_{polar} = \Delta E_{Ele} + \Delta G_{sol-ele}$; $\Delta G_{nonpolar} = \Delta E_{Vdw} + \Delta G_{sol-np}$,$\Delta G_{Bind}$ = estimated total binding free energy.

Complex	ΔE_{Vdw}	ΔE_{Ele}	ΔE_{MM}	$\Delta G_{sol-ele}$	ΔG_{sol-np}	ΔG_{polar}	$\Delta G_{non-polar}$	ΔG_{Bind}
OASS-Met	−17.66	−118.56	−136.22	81.24	−1.28	−37.32	−18.94	−56.27(±7.71)
OASS-Ile	−17.38	−0.85	−18.23	−3.61	−1.33	−4.46	−18.70	−23.17(±6.43)

that PLP rotation is not necessary for active site cleft closure but may be needed for EA formation.

The superimposition of PLP and ligands at the active site from different structures with that of EhOASS-methionine structure reveals only a slight difference in the orientation of the cofactor or ligand with that of EhOASS-methionine structure (Fig. 4). The superimposition of the EhOASS-cysteine bound structure with the EhOASS-methionine structure showed that the cysteine is oriented slightly differently at the active site, making its amino nitrogen atom more accessible to the cofactor PLP Schiff base-forming nitrogen. The distance between these two nitrogen atoms is 2.4 Å for the cysteine bound structure while it is 3.4 Å for the methionine bound structure. This comparison may indicate the different stages of binding of substrate at the active site, where the ligand first binds near the entrance of the active site cleft and then moves towards the cofactor to perform a nucleophilic attack, resulting in the formation of the external Schiff base.

3.4. Analysis of binding interactions and identification of key anchoring residues and hot spot residues using MM/PBSA method

Structural analysis of substrate analog and inhibitor bound structures of OASSs have so far revealed that similar interactions are formed by both these entities to stabilize themselves in the active site, but the trigger which causes switching of the conformation of the enzyme from open to closed has not been identified. The role of Asn 69 of the StOASS 68TNGNT72Asn loop in interacting with methionine has been

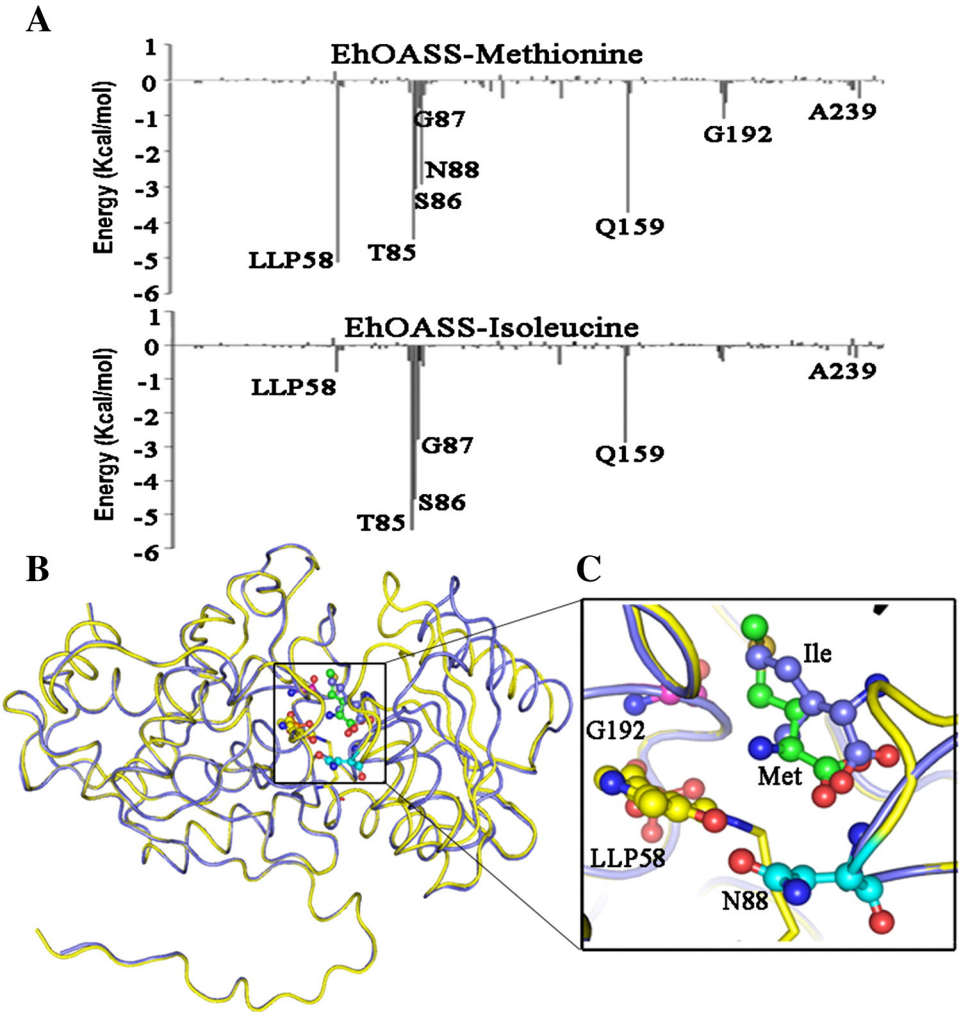

Fig. 5. Per-residue contributions to the binding of different ligands. (A.) Per-residue contributions to the binding of substrate analog, methionine, and inhibitor, isoleucine. Residues of the Asn loop (85TSGNT89) and Gln 159 are the major contributors of binding interactions with both ligands. PLP 58 and Gly 192 are specific major contributors in case of the methionine complex (B.). The overall structure of EhOASS-methionine showing hot spot residues specific for methionine binding to EhOASS is shown in (C.). The hot spot residues are represented in ball and stick model and labeled, pink residue is Gly192, yellow is LLP58 and cyan is Asn88. Methionine bound structure is represented by yellow ribbon and isoleucine bound structure is represented by blue ribbon. Methionine is shown at the active site in green while isoleucine is represented by blue ball and stick model. Inset shows a close up view of the active site with the hot spot residues and ligand.

emphasized [15], but the sequence of this loop is TSGNT in all other OASSs (in EhOASS the equivalent residues are 85TSGNT89), which argues against the general importance of the side chain of this Asn residue (Supplementary Fig. 1). It seems that any residue present at this position would contribute the same interactions with the ligand to stabilize it. We still call it the "Asn loop" as the other Asn (at position 71 in StOASS) is conserved and is also an important contributor to ligand binding.

To shed light on the recognition process, including understanding the differences in the recognition of isoleucine and methionine by EhOASS, binding free energy calculations using MM/PBSA method and decomposition of residue wise energy contribution were carried out. The results also helped us to identify the key residues of EhOASS which are crucial for binding either methionine or isoleucine. A key residue is defined as one that makes at least −1 kcal/mol contribution to the binding free energy. The ΔG_{bind} of the EhOASS-methionine complex was computed to be −56.2 kcal/mol while that for EhOASS-isoleucine complex was found to be −23.2 kcal/mol (Table 3), indicating EhOASS's preference for methionine. The residue level contribution was carried out to extract the key residues involved in the interaction with each of these ligands. The per residue energy profiles for the methionine complex and the isoleucine complex are plotted in Fig. 5A. The important energy contributing residues are also present in the potential H-bonding residues generated from GetNeares and LIGPLOT (Figs. 2C, 3C, 5A and Supplementary Tables 1 and2).

Our calculations indicate that residues T85, S86 and G87 of the Asn loop are important for the recognition of both methionine and isoleucine. They also indicate that LLP58, T193 and Q159 are similarly important, but their contribution to the binding energy differs for the two ligands (Fig. 5A). Whereas LLP58 (PLP bound to catalytic lysine 58) is the key hotspot residue for the binding of methionine, it is only a minor contributor for binding isoleucine. Along with LLP58, the other two hot spot residues in the methionine bound structure different from those in isoleucine bound structure are N88 and G192. N88 is on the flexible N-terminal domain, G192 is present on the rigid C-terminal domain, and LLP58 is the active site center (Fig. 5B); these residues appear to form a triad of energy contributors acting on the bound substrate and resulting in pulling the N-terminal domain closer to the C-terminal domain and closing the active site cleft. The only energy contributing residue variant in the isoleucine bound structure is G87 which is a part of the Asn loop and is on the N-terminal face itself; hence in case of the isoleucine bound structure there is no pull from the C-terminal domain to affect the closure of the active site. The detailed tables of standard deviation of the energetic values are listed in Supplementary Tables 5 & 6.

3.5. Detailed dynamical behaviors of methionine and isoleucine complexes

Structures of EhOASS are available in its native open conformation (2PQM) [8], with the product cysteine bound in the closed conformation (3BM5) [8], and with the methionine substrate analog bound (current work), but we do not have the α-aminoacrylate (αAA) intermediate bound structure. To visualize the conformational changes of OASS along the reaction pathway, we have superimposed onto the native EhOASS structure (Fig. 6A) the two EhOASS-amino acid bound structures (Fig. 6B and D) as well as the MtOASS-αAA structure (2Q3D) [21] (Fig. 6C). As described above, it is only the N-terminal domain which moves to close the active site. The methionine bound structure may be considered to represent the initial interaction of substrate at the active site before the formation of αAA intermediate. As seen in Fig. 6D, the N-terminal domain moves still closer towards the C-terminal domain before releasing the product, cysteine.

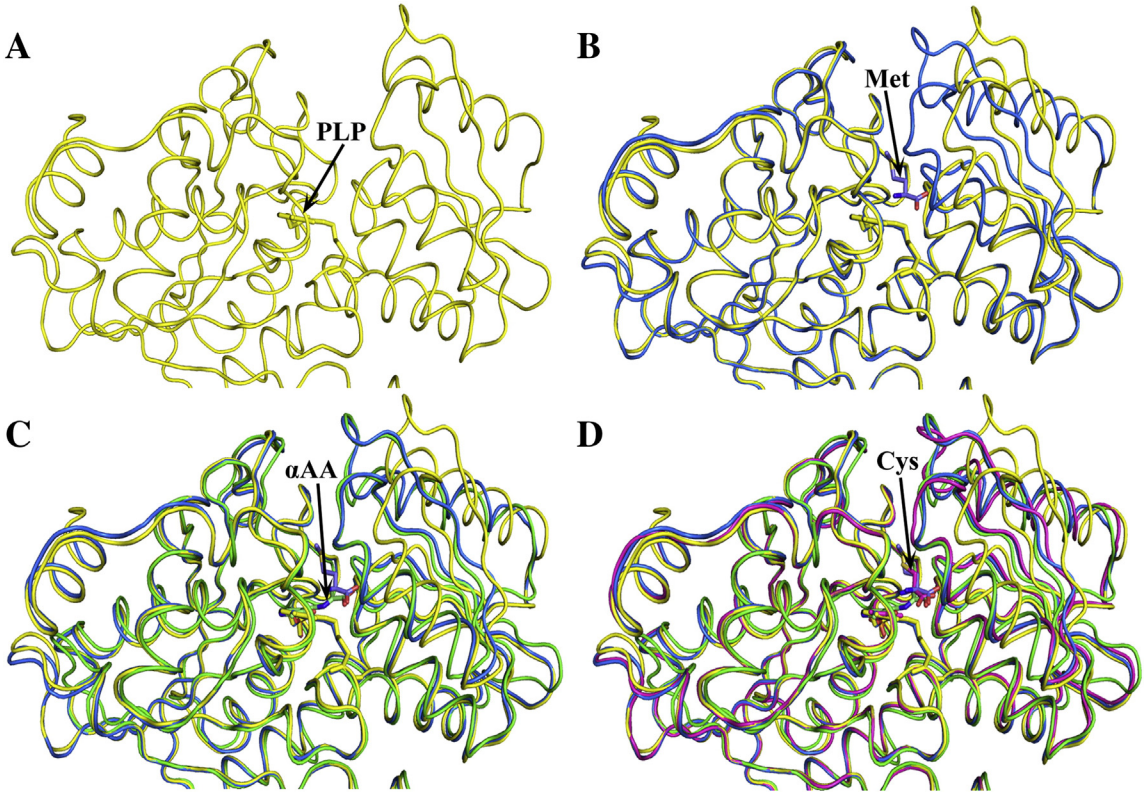

Fig. 6. Conformational changes along the reaction pathway of EhOASS. (A.) Native, open conformation (yellow ribbon) with PLP at the active site. (B.) Substrate analog, methionine, bound closed conformation (blue ribbon) superimposed on the native structure (C.). Reaction intermediate αAA bound MtOASS structure (green ribbon) superimposed on the native structure. The difference seen in C-terminal domain is because of the difference in the structures of the EhOASS and MtOASS proteins and not because of αAA binding. (D.) Structure of EhOASS with bound cysteine product (pink ribbon) superimposed on the native structure. The N-terminal domain moves slightly closer. In all cases the residues of entire monomer were used for superposition.

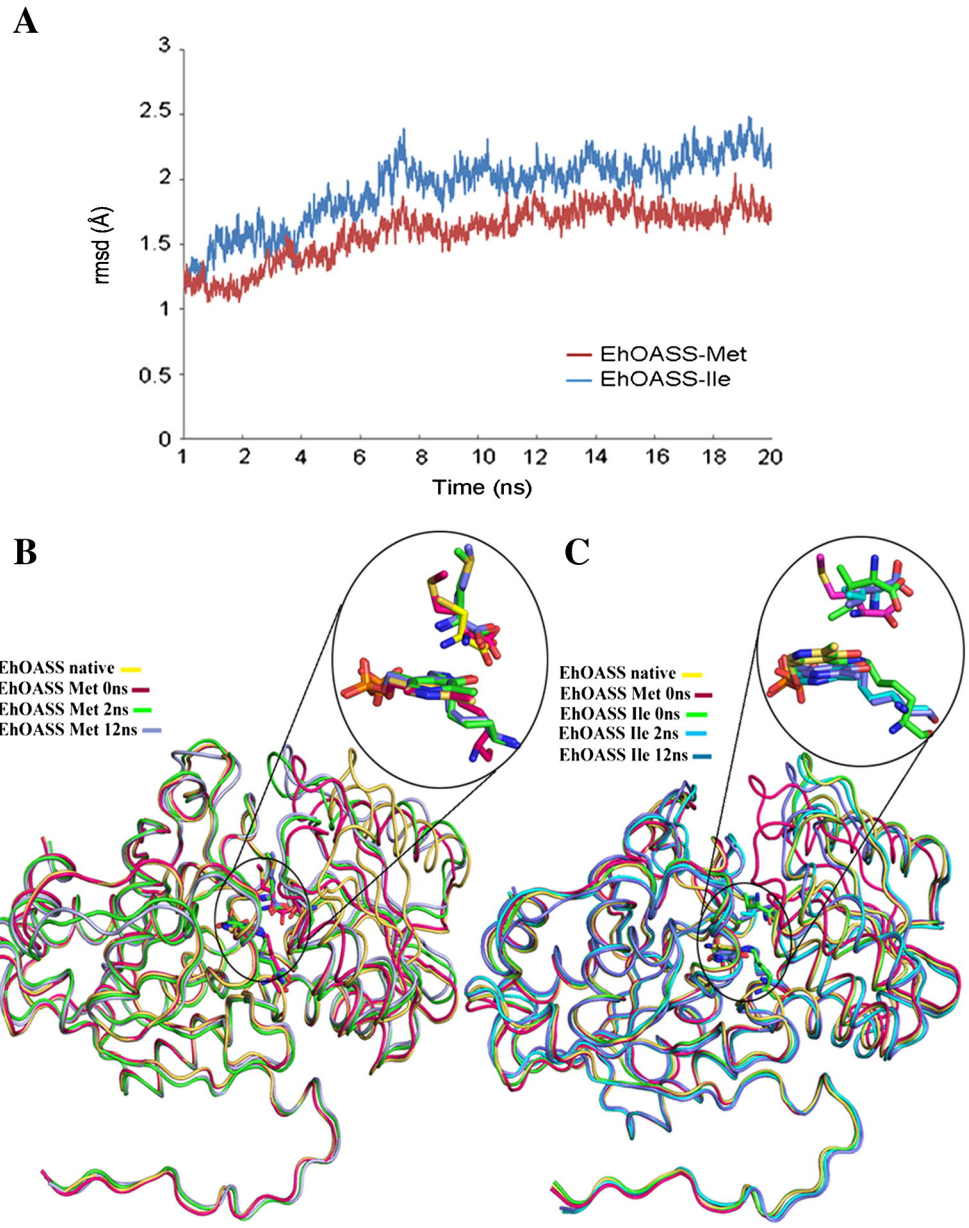

Fig. 7. RMSD analysis and comparison of structural snapshots at various time intervals in the MD trajectories. (A.) Time dependent C_{α}-RMSD analysis of 20 ns MD simulations for EhOASS-methionine and EhOASS-Ile complexes. There are larger variations in case of Ile complex suggesting that the Met complex is relatively more stable. Structural snapshots during the MD trajectories of (B.) methionine bound and (C.) isoleucine bound EhOASS structures. Inset shows the variations in the ligand orientation at equivalent time points.

To determine the specific effect that the binding of each ligand has on the EhOASS structure, and to monitor the conformational changes that occur, the EhOASS-methionine complex and EhOASS-isoleucine complex structures were subjected to MD simulations. The trajectories of both of these MD simulations were stable, with the α-carbon root-mean-square-deviation (RMSD) to the starting structure below 2.5 Å (Fig. 7A). The average backbone RMSD to the final conformation was 1.6 Å and 1.9 Å for the methionine complex and isoleucine complex, respectively (Fig. 7A). The isoleucine bound structure seems to be less stable compared to the methionine bound structure. To understand the finer details of conformational changes at the active site, structural analyses of the MD simulated structures at various time points were carried out. Fig. 7B and C presents the superimposed structural snapshots of Met complex and Ile complex, respectively, at various time points during the MD simulation process. We have chosen the 2 ns and 12 ns structures because these are the time points at which major structural differences in conformation arise in both complexes. As seen in Fig. 7B, the N-terminal domain continues to move to further close the active site. This conformation is maintained until about 12 ns, from which point onward the N-terminal domain starts re-opening. The change in the conformation of the enzyme is accompanied by slight changes in the ligand orientation as revealed in the inset of Fig. 7B. The Schiff base-forming N of methionine continues to move away from PLP as time progresses. For comparison, the cysteine (yellow stick model) from the cysteine-bound structure (3BM5; [8]) is also superimposed over the methionine at the active site. The orientation of the Schiff base-forming N in the cysteine is closer to the equivalent catalytic N of the cofactor PLP, consistent with the slightly more closed active site in this structure compared to the methionine bound structure (Fig. 6D).

The conformational changes observed in the isoleucine complex during the MD trajectory are particularly interesting. Here, the N terminal domain, which is in the open conformation in the crystal structure, nevertheless moves closer to the C-terminal domain in the MD analysis by 4 Å in the first 2 ns and finally to 4.2 Å at 12 ns (Fig. 7C), after which it does not move any further. This change is accompanied

by a change in isoleucine orientation at the active site: the potential Schiff base-forming N of Ile, which faces the opposite direction from catalytic N of the cofactor PLP in the crystal structure, reorients slightly at about 2 ns towards PLP (Fig. 7C inset). This might be triggering the conformational change seen in the N terminal domain. Further reorientation of isoleucine, however, is blocked as bad contacts would arise between the β branching of isoleucine and its own carboxyl group. To test this hypothesis, we computationally mutated methionine to isoleucine in the same conformation, and found that there is a geometrical conflict between the terminal oxygen of the carboxyl group and γ-carbon of the β branching of the isoleucine (Supplementary Fig. 5). Therefore, N-terminal domain movement is restricted at this point and a full closure of the active site is not achieved.

4. Conclusions

The activity of OASS involves the dynamic behavior of the N-terminal domain, which moves to close the active site upon substrate binding. However, the SAT C-terminal peptide acts as inhibitor locking the enzyme in an open conformation. Here, we have examined EhOASS structures in complex with both substrate analog and inhibitor, and identified the key residues and interactions responsible for active site closure. The methionine-bound EhOASS structure shows that cleft can be closed without forming an external aldimine bond, which is in contrast to earlier observations. In all reaction intermediate structures there is a rotation in PLP accompanying ligand binding, whereas in the EhOASS-methionine structure, PLP is rotated by just 1°, indicating that PLP rotation is not needed for cleft closure but may be necessary for external aldimine bond formation. The main driving force behind N-terminal movement and resultant active site closure seems to be the energy contributions by three residues: the cofactor PLP, N88 on the N terminal domain and G192 on the C terminal domain.

On the basis of molecular dynamics studies of methionine bound and isoleucine bound structures, we can now suggest a detailed mechanism for how ligand causes cleft closure. Initially, the carboxyl group of the ligand acts as an anchor and is stabilized at the active site by the residues in N-terminal domain, specially the Asn loop. Then the most important event for substrate binding occurs, i.e., the orientation of Schiff base-forming nitrogen of the substrate towards the nitrogen of cofactor PLP. This appears to trigger the closure of the active site cleft as the nearby residues start contributing energetically favorable interactions, including H-bond formation. Cleft closure depends upon the capacity of the ligand to reorient its amino nitrogen to face the aldimine linkage of LLP. Isoleucine cannot achieve the suitable conformation because of bad contacts between its beta-branched side chain and its own carboxyl group and thus locks the enzyme in an open conformation. An analysis of the binding free energies in both complexes indeed reveals that binding of methionine to EhOASS is more than two fold more favorable than the binding of isoleucine, suggesting methionine to be more stable at the active site then isoleucine.

The results and analyses presented here can be used to improve the design of small molecule drugs aimed at disrupting the activity of OASS in *E. histolytica* and other organisms. Any such inhibitor would act by closing the active site cleft and maintaining it in this conformation, making the active site inaccessible to substrate. So far, the strategy of such work has been based on modeling inhibitors to isoleucine [19,35,36], since isoleucine itself is a known inhibitor. Methionine, however, is shown here to be the stronger binding ligand, since it is a substrate analog which stops the cysteine biosynthetic reaction at the sulfide addition step, it can also act as an inhibitor. Hence, the design of an inhibitor using the methionine complexed closed cleft conformation structure as a template should lead to a more energetically favorable complex compared to isoleucine-based inhibitor molecules which all have binding affinities in micromolar ranges [19,35,36]. We therefore predict that designing drugs based on the methionine bound OASS structure should yield better binding and more effective inhibitors than are currently available.

Acknowledgement

We thank Structural Biology Unit at National Institute of Immunology and Advanced Research Instrumentation facility at Jawaharlal Nehru University for X-ray data collection. We thank Department of Biotechnology BUILDER program and Department of Science and Technology, Govt. of India, for funding. I.R. thanks CSIR for fellowship and M.M. thanks DBT for fellowship.

Appendix A. Supplementary data

Supplementary data to this article can be found online at http://dx.doi.org/10.1016/j.bbagen.2013.05.041.

References

[1] R.C. Fahey, G.L. Newton, B. Arrick, T. Overdank-Bogart, S.B. Aley, *Entamoeba histolytica*: a eukaryote without glutathione metabolism, Science 224 (1984) 70–72.
[2] B.N. Singh, G.P. Dutta, S.R. Das, Effect of O–R potential on the growth and multiplication of axenic *Entamoeba histolytica*, Curr. Sci. 43 (1974) 71–74.
[3] L.S. Diamond, C.C. Cunnick, A serum-free, partly defined medium, PDM-805, for axenic cultivation of *Entamoeba histolytica* Schaudinn, 1903 and other *Entamoeba*, J. Protozool. 38 (1991) 211–216.
[4] F.D. Gillin, L.S. Diamond, Attachment of *Entamoeba histolytica* to glass in a defined maintenance medium: specific requirement for cysteine and ascorbic acid, J. Protozool. 27 (1980) 474–478.
[5] F.D. Gillin, L.S. Diamond, *Entamoeba histolytica* and *Giardia lamblia*: effects of cysteine and oxygen tension on trophozoite attachment to glass and survival in culture media, Exp. Parasitol. 52 (1981) 9–17.
[6] F.D. Gillin, L.S. Diamond, *Entamoeba histolytica* and *Giardia lamblia*: growth responses to reducing agents, Exp. Parasitol. 51 (1981) 382–391.
[7] V.D. Rege, N.M. Kredich, C.H. Tai, W.E. Karsten, K.D. Schnackerz, P.F. Cook, A change in the internal aldimine lysine (K42) in O-acetylserine sulfhydrylase to alanine indicates its importance in transimination and as a general base catalyst, Biochemistry 35 (1996) 13485–13493.
[8] K. Chinthalapudi, M. Kumar, S. Kumar, S. Jain, N. Alam, S. Gourinath, Crystal structure of native O-acetyl-serine sulfhydrylase from *Entamoeba histolytica* and its complex with cysteine: structural evidence for cysteine binding and lack of interactions with serine acetyl transferase, Proteins 72 (2008) 1222–1232.
[9] N.V. Grishin, M.A. Phillips, E.J. Goldsmith, Modeling of the spatial structure of eukaryotic ornithine decarboxylases, Protein Sci. 4 (1995) 1291–1304.
[10] G. Schneider, H. Kack, Y. Lindqvist, The manifold of vitamin B6 dependent enzymes, Structure 8 (2000) R1–R6.
[11] P. Burkhard, G.S. Rao, E. Hohenester, K.D. Schnackerz, P.F. Cook, J.N. Jansonius, Three-dimensional structure of O-acetylserine sulfhydrylase from *Salmonella typhimurium*, J. Mol. Biol. 283 (1998) 121–133.
[12] M.T. Claus, G.E. Zocher, T.H. Maier, G.E. Schulz, Structure of the O-acetylserine sulfhydrylase isoenzyme CysM from *Escherichia coli*, Biochemistry 44 (2005) 8620–8626.
[13] B. Huang, M.W. Vetting, S.L. Roderick, The active site of O-acetylserine sulfhydrylase is the anchor point for bienzyme complex formation with serine acetyltransferase, J. Bacteriol. 187 (2005) 3201–3205.
[14] E.R. Bonner, R.E. Cahoon, S.M. Knapke, J.M. Jez, Molecular basis of cysteine biosynthesis in plants: structural and functional analysis of O-acetylserine sulfhydrylase from *Arabidopsis thaliana*, J. Biol. Chem. 280 (2005) 38803–38813.
[15] P. Burkhard, C.H. Tai, C.M. Ristroph, P.F. Cook, J.N. Jansonius, Ligand binding induces a large conformational change in O-acetylserine sulfhydrylase from *Salmonella typhimurium*, J. Mol. Biol. 291 (1999) 941–953.
[16] J.A. Francois, S. Kumaran, J.M. Jez, Structural basis for interaction of O-acetylserine sulfhydrylase and serine acetyltransferase in the *Arabidopsis* cysteine synthase complex, Plant Cell 18 (2006) 3647–3655.
[17] S. Kumar, I. Raj, I. Nagpal, N. Subbarao, S. Gourinath, Structural and biochemical studies of serine acetyltransferase reveal why the parasite *Entamoeba histolytica* cannot form a cysteine synthase complex, J. Biol. Chem. 286 (2011) 12533–12541.
[18] B. Campanini, F. Speroni, E. Salsi, P.F. Cook, S.L. Roderick, B. Huang, S. Bettati, A. Mozzarelli, Interaction of serine acetyltransferase with O-acetylserine sulfhydrylase active site: evidence from fluorescence spectroscopy, Protein Sci. 14 (2005) 2115–2124.
[19] E. Salsi, A.S. Bayden, F. Spyrakis, A. Amadasi, B. Campanini, S. Bettati, T. Dodatko, P. Cozzini, G.E. Kellogg, P.F. Cook, S.L. Roderick, A. Mozzarelli, Design of O-acetylserine sulfhydrylase inhibitors by mimicking nature, J. Med. Chem. 53 (2010) 345–356.
[20] T. Nozaki, T. Asai, S. Kobayashi, F. Ikegami, M. Noji, K. Saito, T. Takeuchi, Molecular cloning and characterization of the genes encoding two isoforms of cysteine synthase in the enteric protozoan parasite *Entamoeba histolytica*, Mol. Biochem. Parasitol. 97 (1998) 33–44.
[21] R. Schnell, W. Oehlmann, M. Singh, G. Schneider, Structural insights into catalysis and inhibition of O-acetylserine sulfhydrylase from *Mycobacterium tuberculosis*. Crystal structures of the enzyme alpha-aminoacrylate intermediate and an enzyme-inhibitor complex, J. Biol. Chem. 282 (2007) 23473–23481.

[22] I. Raj, S. Kumar, S. Gourinath, The narrow active-site cleft of O-acetylserine sulfhydrylase from *Leishmania donovani* allows complex formation with serine acetyltransferases with a range of C-terminal sequences, Acta Crystallogr. D: Biol. Crystallogr. D68 (2012) 909–919.
[23] C. Krishna, R. Jain, T. Kashav, D. Wadhwa, N. Alam, S. Gourinath, Crystallization and preliminary crystallographic analysis of cysteine synthase from *Entamoeba histolytica*, Acta Crystallogr. F Struct. Biol. Cryst. Commun. 63 (2007) 512–515.
[24] K.S. Bartels, C. Klein, Automar, in, vol. 2.8, Marresearch MAR Research GmbH, 2010.
[25] A. Vagin, A. Teplyakov, MOLREP: an automated program for molecular replacement, J. Appl. Crystallogr. 30 (1997) 1022–1025.
[26] G.N. Murshudov, A.A. Vagin, E.J. Dodson, Refinement of macromolecular structures by the maximum-likelihood method, Acta Crystallogr. D: Biol. Crystallogr. 53 (1997) 240–255.
[27] P. Emsley, K. Cowtan, Coot: model-building tools for molecular graphics, Acta Crystallogr. D: Biol. Crystallogr. 60 (2004) 2126–2132.
[28] D.A. Case, T.A. Darden, C.L. Simmerling Cheatham, J. Wang, R.E. Duke, R. Luo, K.M. Merz, D.A. Pearlman, M. Crowley, R.C. Walker, W. Zhang, B. Wang, S. Hayik, A. Roitberg, G. Seabra, K.F. Wong, F. Paesani, X. Wu, S. Brozell, V. Tsui, H. Gohlke, L. Yang, C. Tan, J. Mongan, V. Hornak, G. Cui, P. Beroza, D.H. Mathews, C. Schafmeister, W.S. Ross, P.A. Kollman, Amber 9 University of California, San Francisco, 2006.
[29] J. Wang, R.M. Wolf, J.W. Caldwell, P.A. Kollman, D.A. Case, Development and testing of a general amber force field, J. Comput. Chem. 25 (2004) 1157–1174.
[30] M.C. Lee, Y. Duan, Distinguish protein decoys by using a scoring function based on a new Amber force field, short molecular dynamics simulations, and the generalized born solvent model, Proteins 55 (2004) 620–634.
[31] T. Darden, L. Perera, L. Li, L. Pedersen, New tricks for modelers from the crystallography toolkit: the particle mesh Ewald algorithm and its use in nucleic acid simulations, Structure 7 (1999) R55–R60.
[32] P.A. Kollman, I. Massova, C. Reyes, B. Kuhn, S. Huo, L. Chong, M. Lee, T. Lee, Y. Duan, W. Wang, O. Donini, P. Cieplak, J. Srinivasan, D.A. Case, T.E. Cheatham III, Calculating structures and free energies of complex molecules: combining molecular mechanics and continuum models, Acc. Chem. Res. 33 (2000) 889–897.
[33] K. Mino, T. Yamanoue, T. Sakiyama, N. Eisaki, A. Matsuyama, K. Nakanishi, Effects of bienzyme complex formation of cysteine synthetase from *Escherichia coli* on some properties and kinetics, Biosci. Biotechnol. Biochem. 64 (2000) 1628–1640.
[34] E. Salsi, B. Campanini, S. Bettati, S. Raboni, S.L. Roderick, P.F. Cook, A. Mozzarelli, A two-step process controls the formation of the bienzyme cysteine synthase complex, J. Biol. Chem. 285 (2010) 12813–12822.
[35] L. Amori, S. Katkevica, A. Bruno, B. Campanini, P. Felici, A. Mozzarelli, G. Costantino, Design and synthesis of trans-2-substituted-cyclopropane-1-carboxylic acids as the first non-natural small molecule inhibitors of O-acetylserine sulfhydrylase, Med. Chem. Commun. 3 (2012) 1111–1116.
[36] I. Nagpal, I. Raj, N. Subbarao, S. Gourinath, Virtual screening, identification and in vitro testing of novel inhibitors of O-acetyl-L-serine sulfhydrylase of *Entamoeba histolytica*, PLoS One 7 (2012) e30305.